CORROSION SCIENCE AND TECHNOLOGY, Vol.15, No.3(2016), pp.120~124 pISSN: 1598-6462 / eISSN: 2288-6524
DOI: http://dx.doi.org/10.14773/cst.2016.15.3.120

Role of Ca in Modifying Corrosion Resistance and Bioactivity of Plasma Anodized AM60 Magnesium Alloys

Anawati Anawati[1], Hidetaka Asoh[1,2], and Sachiko Ono[1,2,†]

[1]*Research Institute for Science and Technology*
[2]*Department of Applied Chemistry, Kogakuin University, 2665-1 Nakano, Hachioji, Tokyo 192-0015, Japan*

(Received January 28, 2016; Revised June 26, 2016; Accepted June 26, 2016)

The effect of alloying element Ca (0, 1, and 2 wt%) on corrosion resistance and bioactivity of the as-received and anodized surface of rolled plate AM60 alloys was investigated. A plasma electrolytic oxidation (PEO) was carried out to form anodic oxide film in 0.5 mol dm^{-3} Na_3PO_4 solution. The corrosion behavior was studied by polarization measurements while the in vitro bioactivity was tested by soaking the specimens in Simulated Body Fluid (1.5xSBF). Optical micrograph and elemental analysis of the substrate surfaces indicated that the number of intermetallic particles increased with Ca content in the alloys owing to the formation of a new phase Al_2Ca. The corrosion resistance of AM60 specimens improved only slightly by alloying with 2 wt% Ca which was attributed to the reticular distribution of Al_2Ca phase existed in the alloy that might became barrier for corrosion propagation across grain boundaries. Corrosion resistance of the three alloys was significantly improved by coating the substrates with anodic oxide film formed by PEO. The film mainly composed of magnesium phosphate with thickness in the range 30 - 40 μm. The heat resistant phase of Al_2Ca was believed to retard the plasma discharge during anodization and, hence, decreased the film thickness of Ca-containing alloys. The highest apatite forming ability in 1.5xSBF was observed for AM60-1Ca specimens (both substrate and anodized) that exhibited more degradation than the other two alloys as indicated by surface observation. The increase of surface roughness and the degree of supersaturation of 1.5xSBF due to dissolution of Mg ions from the substrate surface or the release of film compounds from the anodized surface are important factors to enhance deposition of Ca-P compound on the specimen surfaces.

Keywords : *magnesium, biodegradable, bioactivity, anodization, corrosion.*

1. Introduction

During the last decade, there has been a great interest in investigating Mg and its alloys for application as temporary implant materials in cardiovascular and orthopaedic devices[1-6]. This is due to the unique property of Mg that degrades spontaneously in physiological solutions and due to the proximity of the mechanical properties to that of the natural bone[1]. The dissolved ions are tolerable for human body system and even beneficial for some metabolic reactions[7]. However, its application was limited due to the relatively poor corrosion resistance of Mg when exposed to human body fluid. Consequently, the implant will liberate strong hydrogen gas and cause loss of mechanical integrity before the replaced tissue or bone completely heals.

Great efforts have been done to improve the corrosion resistance by alloying, surface treatment, and coating[1-5]. Conventional Mg alloys (AZ and AM) commonly used Al as the main alloying element that could enhance the corrosion resistance and mechanical properties of Mg alloys[2,3,5,6]. Implant devices such as screws and pins used to fix bone fracture, are expected to handle tension and compression stresses during service. Therefore, Mg is preferably used in the alloys form. AZ31 and AZ91 are mostly studied magnesium alloys but there is only few reports in exploring AM (containing Al and Mn) Mg series alloys for biodegradable materials. Small amounts of Mn are tolerable and essential in the human body[3]. In fact, addition of small amount of Mn is a commercial way of mitigating the detrimental effect of impurities thus improving corrosion resistance[3,8].

Ca is another interesting alloying element that had been explored for Mg based alloys. It was reported[3,4,5,9] that Ca enhanced the corrosion resistance and mechanical properties of Mg alloys. Ca can be tolerated by human

† Corresponding author: sachiono@cc.kogakuin.ac.jp

body[3]. It is a major component in human bone and essential in chemical signalling with cells[10]. However, most of the reported works were focused on the effect of Ca on microstructure, mechanical properties and corrosion behavior[3,4,5,9] of the substrate. There has been lack of reports on the effect of alloying element Ca on anodic oxide film characteristics formed on Mg alloys. In this work, the effect of alloying element Ca on the corrosion resistance and apatite forming ability (bioactivity) of the anodic oxide film formed by plasma electrolytic oxidation (PEO) on AM60 magnesium alloy was investigated.

2. Experimental Procedure

The specimens used were rolled plates of commercial AM60 magnesium alloys with Ca content 0, 1, and 2 wt%. The chemical composition of the AM60 alloy is listed in Table 1. The specimen was cut into pieces to give a working area of 5 cm^2 with thickness of 1 mm. For microstructure observation, the specimens were ground to #1200 grit paper. The surface microstructure was studied by optical microscope (Olympus BX51M type).

Prior to anodization, pretreatment was applied in a mixed acid solution of 8 vol% HNO_3-1 vol% H_3PO_4 for 20 s and then washed with deionized (DI) water before dipping in 5 wt% NaOH solution at 80 °C for 1 min. Anodizing was carried out by plasma electrolytic oxidation technique in 0.5 $moldm^{-3}$ Na_3PO_4 solution at a constant current of 200 Am^{-2} at 25 °C for 20 min. The oxide film thickness was measured by using a coating thickness meter of dual type (SME-1) from Sanko.

The corrosion behavior of the specimens was investigated by polarization test in physiological solution 0.9 wt% NaCl solution at 37 °C based on ASTM standard and our earlier work[11]. The polarization test was performed by using a potentiostat instrument from IviumStat started from potential -1.65 $V_{Ag/AgCl}$ and terminated when the current output reach 30 mA at a sweep rate 1 mV s^{-1}. The polarization measurement was conducted immediately upon immersion of the specimen in the test solution. Pt wire was used as a counter electrode and silver chloride was used as a reference electrode. The corrosion potential and current densities were determined by Tafel plot.

The apatite forming ability of the specimens was evaluated by an *in-vitro* test in 1.5SBF with 1.5 times of concentration of SBF10 for 7 days. The SBF10 was prepared as previously reported[12]. The solution pH was adjusted to 7.4 at 36.4 °C. Sodium azide (NaN_3) was added to the resulting solution to inhibit bacterial growth. The specimens were exposed to the solution with a surface-to-volume ratio of 20 ml cm^{-2}. The solution was refreshed after 3 days. After the test, the specimen was rinsed thoroughly with DI water and then dried in air stream.

The elemental analysis was performed by using an energy dispersive X-ray spectroscopy (EDS, JEOL EX-54175JMU) attached to SEM (JEOL JSM-6380LA).

3. Results and Discussion

Fig. 1 shows the optical microscope images showing the microstructure of the three alloys. The base alloy exhibited grain sizes in the range of 10 - 50 μm (Fig. 1a).

Table 1. Chemical composition of AM60 alloy in wt%

Mg	Al	Zn	Mn	Cu	Ni	Si	Be
Bal.	5.6	≤ 0.2	0.26	≤ 0.008	≤ 0.001	≤ 0.08	≤ 0.0005

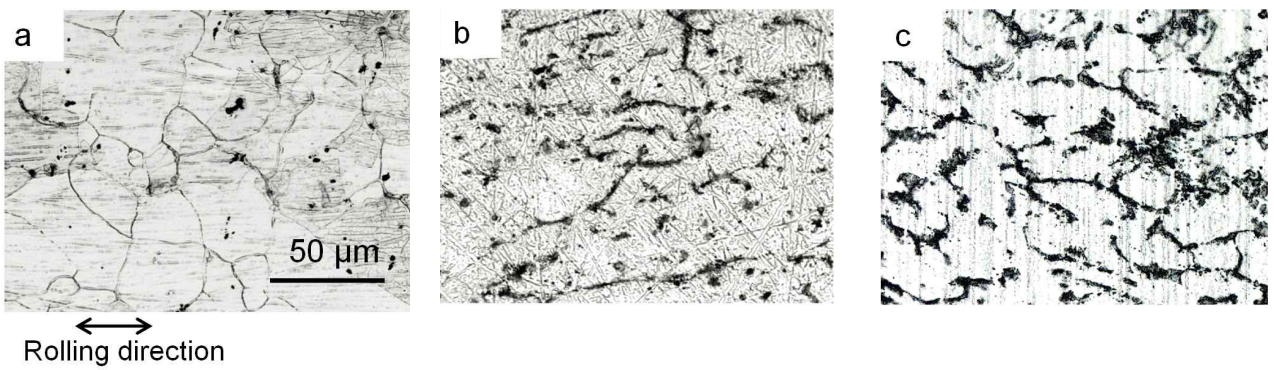

Fig. 1. The optical micrographs of a) AM60, b) AM60-1Ca, and c) AM60-2Ca alloys. The scale bar and rolling direction in a) apply to all images. The coarse lines appeared in image b) and c) were the grinding lines.

Addition of 1 and 2 wt% Ca in the alloy did not affect the grain sizes significantly but it modified the composition and the number of intermetallic particles. Similar as previously reported[8,9], the microstructure of AM60 was composed of α-Mg matrix and β-$Mg_{17}Al_{12}$ as analyzed by EDS. A new phase of Al_2Ca was formed along grain boundaries when Ca was present in the alloys. The number of Al_2Ca phases increased with Ca content in the alloys. Some of these phases appeared continuous along grain boundaries while others existed as spheroidized particles (Fig. 1b). The grains of AM60-1Ca were coarser compare to those of the other two alloys. In the alloy containing 2 wt% Ca, the Al_2Ca phases became more continuous and formed a network (Fig. 1c). Formation of Al_2Ca phases was attributed to the low solubility of Ca in Mg. The equilibrium phase diagram indicated that the maximum solid solubility of Ca in Mg is 0.82 at %[13]. Above the solubility limit, the excess of Ca was assumed to dissolve in the intermetallics by replacing Mg in β-$Mg_{17}Al_{12}$ to form Al_2Ca phase[5,9]. The Al_2Ca network formed in AM60-2Ca was beneficial to stop the corrosion propagation of localized attack into adjacent grains[8]. The polarization measurements indicated that the current densities of AM60 alloys decreased gradually by increasing Ca content in the alloys as tabulated in Table 1. The effect of Ca on corrosion potential was only observed on AM60-2Ca which exhibited higher corrosion potentials of -1.55 $V_{Ag/AgCl}$ than that of the other two alloys (-1.57 $V_{Ag/AgCl}$).

Anodization of the three alloys for 20 min resulted in the formation of porous oxide film with average thickness of 42 μm, 36 μm, and 35 μm for AM60, AM60-1Ca, and AM60-2Ca specimens, respectively. The film thickness decreased with increasing Ca content in the alloys owing to the increase number of Al_2Ca phase in the alloys. The Al_2Ca phase is a heat resistant phase and a stable line compound with a relatively high melting point[14]. The presence of Al_2Ca phase delayed the appearance of a big sparks/plasma which responsible for the rapid thickening of the oxide film. However, since the type of film was porous, thicker oxide did not necessarily provide better corrosion protection. The film density and composition are more important properties that affect the corrosion behavior of anodized specimen. The oxide film composed of magnesium phosphate regardless of Ca content in the alloy, as analyzed by EDS. The anodic film formed on the three alloys greatly enhanced the corrosion resistance during polarization test in NaCl solution as indicated by lower corrosion current density down to two order of magnitude relative to the substrates (Fig. 2). The corrosion potential and corrosion current densities values are listed in Table 2. The corrosion potential of anodized AM60-1Ca specimen was nearly similar as of the substrate while slight increase of corrosion potential was obtained for anodized AM60 compare to the substrate. Combination of the noblest corrosion potential and the lowest corrosion current density was obtained for anodized specimen of AM60-2Ca alloy as well as the substrate itself as compare to the other two alloys. The relatively small differences in corrosion potential when comparing the three alloys in both substrate and anodized condition is due to the fact that the potential is more a representative of the corroding solid solution matrix than of the intermetallics[8].

The apatite forming ability of the substrates and the anodized specimens were analyzed after SBF soaking for

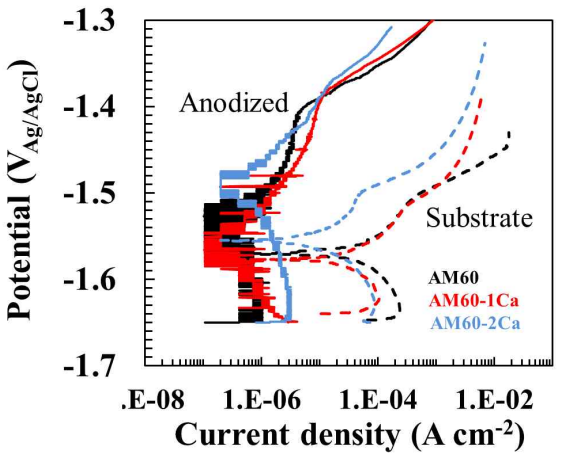

Fig. 2. Potentiodynamic polarization of substrate and anodized AM60, AM60-1Ca, and AM60-2Ca in 0.9% NaCl solution.

Table 2. Corrosion potentials ($V_{Ag/AgCl}$) and current densities (A cm^{-2}) data obtained from polarization measurements in 0.9 wt% NaCl solution of the three alloys in both substrate and anodized form

Specimen		Substrate	Anodized
AM60	E_{corr}	-1.57	-1.54
	i_{corr}	2.20 x 10^{-5}	5.11 x 10^{-7}
AM60-1 Ca	E_{corr}	-1.57	-1.56
	i_{corr}	1.96 x 10^{-5}	4.15 x 10^{-7}
AM60-2 Ca	E_{corr}	-1.55	-1.48
	i_{corr}	8.20 x 10^{-6}	5.11 x 10^{-7}

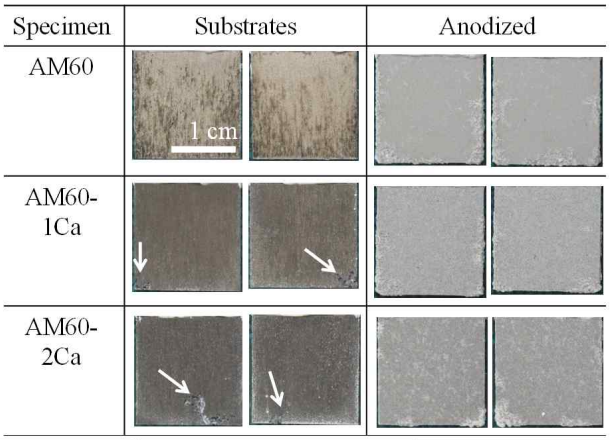

Fig. 3. The specimen's appearance of both surfaces of substrates and anodized specimens after soaking in 1.5SBF for 7 days. The scale bar in a) applies to all images.

7 days. The specimen's appearances on both sides of surfaces of substrates and anodized specimens after SBF soaking are shown in Fig. 3. All of the substrates surfaces (left sides) had been attacked by a relatively uniform corrosion. Only few pits, indicated by arrows in Fig. 3, were observed near the edges of the Ca-containing specimens. The corroded surfaces of AM60 substrate showed variation of whitish and dark-grey areas while the Ca-containing alloys were uniformly dark-grey. The discoloration suggested variation in the deposit layer composition. The dark-grey areas apparently propagated preferentially along the rolling lines vertically from the lower part of the specimen's edge towards the upper part of the specimen visible as dark-grey furrows in Fig. 3 (AM60 substrate). EDS analysis on the surface layers of the three specimens over an area of 650 μm x 485 μm detected similar elements composition of Mg, O, Cl, Ca and P. The O concentration was almost similar about 50 mass% for the three alloys while Cl concentration decreased with increasing Ca content in the alloys, 1.18, 0.53, and 0.36 mass% for the AM60, AM60-1Ca, and AM60-2Ca alloys, respectively. The Ca and P concentrations were plotted and shown in Fig. 4. The EDS elemental analysis indicated that the whitish areas corresponded to the corroded areas covered mainly by corrosion product of $Mg(OH)_2$ and $MgCl_2$. The $Mg(OH)_2$ layer gave a typical white dull appearance[8]. The dark-grey areas were also corroded areas but covered by additional Ca-P compounds.

Fig. 4 shows the quantitative EDS analysis results of the substrate surfaces after SBF soaking for 7 days. The graph plotted the concentrations of Ca and P which are the main elements of apatite. It is obvious that higher Ca and P concentrations were obtained on the Ca-containing alloys indicating higher deposition of Ca-P compound on the surfaces, than that on the base alloy. The Ca concentration of the substrate surfaces notably increased from 4.7 to 15.4 mass% by addition of 1 wt% Ca in the alloys. The Ca concentration further increased slightly to 17.6 mass% on 2 wt% Ca-containing alloy surface while the P concentration was relatively similar at 14.0 mass%. Thus, it is concluded that the deposit layer formed on Ca-containing alloys was highly contained Ca-P compounds rather than $Mg(OH)_2$ or $MgCl_2$ phases. The $Mg(OH)_2$ layer which formed initially was probably decomposed into Ca-P compounds. The absence of whitish areas in Ca-containing alloys indicated uniform deposition of Ca-P compounds on the surface while only local deposition was observed on the AM60 substrate.

The corrosion resistance of anodized specimens in 1.5xSBF is better than of the substrates. All of the anodized specimens show no visible corroded areas or pit (Fig. 3). The surface appearance of anodized specimens after SBF immersion was similar to those before immersion.

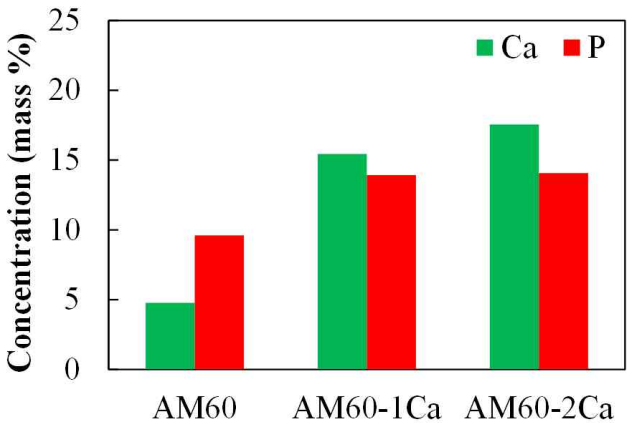

Fig. 4. Concentration (mass %) of Ca and P of the substrates after SBF soaking for 7 days.

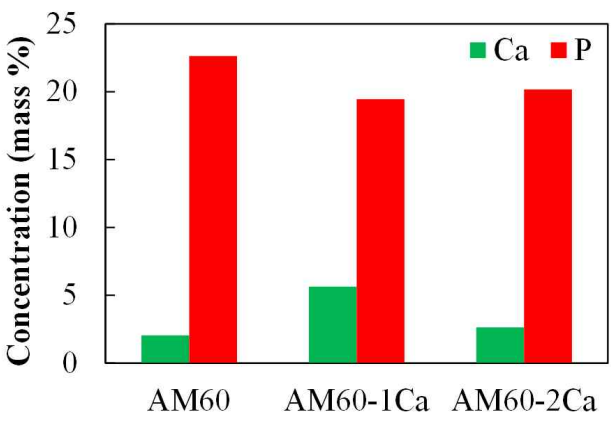

Fig. 5. Concentration (mass%) of Ca and P of the anodized specimens after SBF soaking for 7 days.

The results of immersion test on anodized specimens were in agreement with the polarization data that indicated an improvement in corrosion resistance by anodization. However, the apatite forming ability of the anodic film was relatively low. Fig. 5 shows the obtained Ca and P concentrations of the anodized specimens after SBF immersion. The high P concentration stems from the film which composed of magnesium phosphate. The highest Ca concentration (7.4 mass%) was obtained on the film formed on AM60-1Ca alloy followed by AM60-2Ca alloy. SEM investigation on the surface after SBF immersion indicated a superficial dissolution of the anodic film surfaces had occurred on the film formed on AM60-1Ca alloy while the film formed on the other two alloys remained intact. The release of oxide film component such as phosphate to the solution may increase the degree of supersaturation of 1.5xSBF relative to apatite[1,2,4,6] and therefore triggered higher deposition of Ca-P compound on the film surface of AM60-1Ca alloy. Another factor is the increase of surface roughness which became preferential site for Ca-P compound deposition.

4. Conclusions

Addition of alloying element Ca modified the microstructure, corrosion behaviour in NaCl solution, and bioactivity in 1.5SBF of AM60 alloys in both substrate and anodized specimens. Al_2Ca phase was formed along grain boundaries and the number phase increased with Ca content in the alloys. The presence of heat resistant Al_2Ca phase delayed the initiation of big sparks during anodizing and hence decreased the film thickness. The network of Al_2Ca phase existed in AM60-2Ca enhanced the corrosion resistance of the specimens both substrate and anodized during polarization in NaCl solution. The AM60-1Ca specimens of both substrate and anodized exhibited higher apatite forming ability than the other two alloys. The reason was due to higher dissolution of substrate or anodized surfaces experienced by this alloy which further contributed to the increase in the degree of supersaturation of the solution relative to the apatite and the increase in surface roughness that triggered deposition of Ca-P compound on the surface.

Acknowledgments

We acknowledge the Light Metal Educational Foundation, Inc., and the Ministry of Education, Culture, Sports, Science and Technology of Japan (MEXT)-Supported Program for the Strategic Research Foundation at Private Universities, 2013-2017.

References

1. L. C. Li, J. C. Gao, Y. Wang, *Surf. Coat. Tech.*, **185**, 92 (2004).
2. F. Witte, V. Kaese, H. Haferkamp, E. Switzer, A. Meyer-Lindberg, C. J. Wirth, H. Windhagen, *Biomaterials*, **26**, 3557 (2005).
3. G. Song, *Corros. Sci.*, **49**, 1696 (2007).
4. Z. Li, X. Gu, S. Lou, Y. Zheng, *Biomaterials*, **29**, 1329 (2008).
5. M. B. Kannan, R. K. S. Raman, *Biomaterials*, **29**, 2306 (2008).
6. S. Virtanen, *Mater. Sci. Eng. B,* **176**, 1600 (2011).
7. J. Vormann, *Mol. Aspects Med.*, **24**, 27 (2003).
8. O. Lunder, *Corrosion Rev.*, **15**, 439 (1997).
9. B. Kondori, R. Mahmudi, *Mater. Sci. Eng. A*, **527**, 2014 (2010).
10. J. Z. Ilich, J. E. Kerstetter, *J. Am. Coll. Nutr.*, **19**, 715 (2000).
11. Anawati, H. Tanigawa, H. Asoh, S. Ono, *Corros. Sci.*, **70**, 212 (2013).
12. L. Müller, F. A. Müller, *Acta Biomater.* **2**, 181 (2006).
13. A. A. Nayeb-Hashemi, J. B. Clark, *Bulletin of Alloy Phase Diagrams,* **8**, 58 (1987).
14. H. I. Kaplan, J. Hryn and B. Clow, *Magnesium Technology 2000*, p. 279 (TMS, 2000).